Analytical and numerical adjoint solutions for cumulative streamflow depletion

Chris Turnadge[1*], Roseanna M. Neupauer[2], Okke Batelaan[3], Russell S. Crosbie[1], Craig T. Simmons[3]

[1] CSIRO Land and Water, Locked Bag 2, Glen Osmond, SA 5064, Australia.

[2] Department of Civil, Environmental and Architectural Engineering, University of Colorado, Boulder, CO 80309, USA.

[3] National Centre for Groundwater Research and Training, Flinders University, GPO Box 2100, Adelaide, SA 5001, Australia.

* Corresponding author: Chris Turnadge (Chris.Turnadge@csiro.au)

Key Points:

- A new numerical adjoint solution for cumulative streamflow depletion was derived
- A new analytical solution for cumulative streamflow depletion was derived
- The derived adjoint solution can be orders of magnitude more efficient than traditional perturbation-based approaches to estimating cumulative streamflow depletion

Abstract

The traditional metric of streamflow depletion represents the instantaneous change in the volumetric rate of aquifer–stream exchange after a finite period of continuous groundwater extraction. In the present study an alternative metric of streamflow depletion was considered: cumulative stream depletion (CSD), which described the total volumetric reduction in flow from an aquifer to a stream resulting from continuous groundwater extraction over a finite period, at the final time of extraction. A novel analytical solution for the prediction of CSD was derived,

based upon a forward solution that accounted for streambed conductance and partial stream penetration. Separately, a novel numerical solution for prediction of CSD was derived, based on the derivation and calculation of an adjoint state solution. The accuracy of these methods was demonstrated through benchmarking against existing analytical solutions and perturbation-based results, respectively. The derivation of the adjoint state solution identified three parameters of relevance to CSD prediction: streambed hydraulic conductivity and thickness, both of which contribute to the lumped parameterization of streambed conductance, as well as aquifer specific yield, which controls the rate at which hydraulic perturbations propagate through an aquifer. The computational advantage of the numerical adjoint solution was highlighted, where a single numerical model can be used to predict CSD resulting from any potential groundwater extraction location. The reduction in computational time required was proportional to the number of potential extraction well locations. If the number of potential locations is large then a reduction in model run time of nearly 100 % can be achieved.

1. Introduction

The concept of streamflow depletion typically describes a reduction in flow between an aquifer and a connected, gaining stream resulting from groundwater extraction (Barlow and Leake, 2012). This concept can be generalised to losing streams, where increases in stream discharge may occur, as well as to other surface water features such as rivers and lakes. Streamflow depletion can result in the reduction or cessation of aquifer–stream exchange fluxes. Where streams provide potable water supplies for municipal, domestic or agricultural uses, reductions in baseflow can put the security of such supplies at risk. Reductions to in-stream flow regimes and the resulting changes to water chemistry can also cause considerable negative ecological impacts.

1.1. Instantaneous streamflow depletion

Traditionally, streamflow depletion metrics were conceptualized as the reduction in groundwater discharge to a stream (Q_S) resulting from continuous groundwater extraction at a rate, Q_B, over a finite period (e.g. from t_0 to t_f), at the final time of extraction (t_f); i.e.:

$$Q_{ISD}(t_f) = \Delta Q_S = \frac{dQ_S(t_f)}{dQ_B} Q_B \tag{1}$$

where $Q_{ISD}(t_f)$ is instantaneous streamflow depletion (ISD) with volumetric flow rate units. Alternatively, other studies used the ratio of ISD to volumetric extraction rate, which is unitless. Interactions between an unconfined aquifer and a stream can be conceptualized in various ways. The simplest approach involves calculating the exchange flow at a given time $Q_S(t)$ as a function of the difference between aquifer hydraulic head, h, and stream stage, h_S; i.e.:

$$Q_S(t) = \int_{\Omega} C_S(\mathbf{x}) \, [h(\mathbf{x},t) - h_S(\mathbf{x},t)] \, A_S(\mathbf{x}) \, d\mathbf{x} \tag{2}$$

where A_S is a dimensionless function that has a value of unity along streams and zero elsewhere, and C_S is a lumped parameter known as streambed conductance [L.T^{-1}], defined as:

$$C_{S(\mathbf{x})} = \frac{K_S(\mathbf{x}) \, W_S(\mathbf{x})}{b_S(\mathbf{x})} \tag{3}$$

where K_S is streambed hydraulic conductivity [L.T^{-1}], W_S is streambed width perpendicular to flow [L], and b_S is streambed thickness parallel to flow [L]. The inclusion of the term A_s in equation (2) ensures that, while integration is performed over the domain of interest, stream–aquifer exchange occurs only at stream locations. When numerical solution methods are used, appropriate specification of the terms W_S and b_S is necessary to ensure accurate prediction of streamflow depletion (Mehl and Hill, 2010). Streambed conductance values can be estimated through inversion of simultaneous observations of stream flow, stream stage, and aquifer hydraulic head. Alternatively, the component parameters of the streambed conductance term can be estimated independently using laboratory testing methods, such as streambed sediment particle size distribution analyses (Fox et al., 2011), or from field observations, such as falling head permeameter testing (Landon et al., 2001; Fox, 2004). Existing analytical and numerical methods of estimating ISD are summarized as follows.

1.2. Analytical solutions for instantaneous streamflow depletion

A vast number of analytical and semi-analytical solutions for the first-order prediction of ISD have been developed since the 1940s (Hunt, 2014; Huang et al., 2018), of which a handful have seen widespread uptake. The seminal ISD solution was derived by Theis (1941), the calculation of which was subsequently simplified by Glover and Balmer (1954). This solution featured a relatively large number of assumptions, including: the absence of a streambed conductance layer; that the stream and bore both fully penetrate the aquifer; that hydraulic properties are homogeneous; and that extraction is continuous.

Theis (1941) and Glover and Balmer (1954) presented a closed-form analytical solution for the estimation of depletion of unconfined groundwater flow to a fully connected, fully penetrating stream featuring no resistance to flow (i.e. zero streambed thickness). Theis (1941) extended the Theis (1935) drawdown solution via the inclusion of an infinitely long Dirichlet boundary condition of infinitesimal width to represent a stream boundary. At the time of publication, the complementary error function had not been defined; therefore, the Theis (1941) solution was written in terms of a definite integral that required numerical evaluation. Glover and Balmer (1954) later derived a true closed-form solution using the complementary error function, which was by then widely available (Hunt, 2014). This conceptualization will hereafter be referred to as the “TGB solution”. The TGB solution describes instantaneous streamflow depletion (Q_{ISD}) at time t resulting from continuous groundwater extraction from time zero to time t as:

$$Q_{ISD}(t) = Q_B \operatorname{erfc}\left[\sqrt{\frac{(\Delta x)^2 \, S_y}{4 \, T \, t}}\right] \tag{4}$$

where Δx is bore-stream separation distance (L), t is the duration of time elapsed since the onset of groundwater extraction (T), T is unconfined aquifer transmissivity ($L^2.T^{-1}$), S_y is unconfined aquifer storage coefficient (unitless) and erfc is the complementary error function. In practice, specific yield values are used to parameterize the latter term, while a constant aquifer thickness is used to calculate an appropriate T value. Importantly, this requires the assumption that reductions in aquifer saturated thickness due to extraction (i.e. drawdowns) are negligible with respect to total aquifer thickness.

Hantush (1965) extended the TGB solution to include a relatively lower hydraulic conductivity conductance layer between the pumped aquifer and the stream (i.e. non-zero streambed thickness). The remainder of the assumptions used by the TGB solution were retained, including full aquifer penetration of both the production bore and stream. This conceptualization will hereafter be referred to as the “Hantush solution”. The Hantush solution described instantaneous streamflow depletion at time t resulting from continuous groundwater extraction as:

$$Q_{ISD}(t) = Q_B \left\{ \operatorname{erfc}\left[\sqrt{\frac{(\Delta x)^2 \, S_y}{4 \, T \, t}}\right] - \exp\left[\frac{T \, t}{S_y \, R^2} + \frac{\Delta x}{R}\right] \operatorname{erfc}\left[\sqrt{\frac{T \, t}{S_y \, R^2}} + \sqrt{\frac{(\Delta x)^2 \, S_y}{4 \, T \, t}}\right] \right\} \tag{5}$$

where $R = K \, b_S \, / \, K_S$.

Hunt (1999) later derived a solution that accounted for the effects of a stream bed conductance layer, a partially penetrating stream, and a partially penetrating bore. This conceptualization will hereafter be referred to as the "Hunt solution". The Hunt solution described instantaneous streamflow depletion at time t resulting from continuous groundwater extraction as:

$$Q_{ISD}(t) = Q_B \left\{ \operatorname{erfc}\left[\sqrt{\frac{(\Delta x)^2 S_y}{4\,T\,t}}\right] - \exp\left[\frac{\lambda^2 t}{4\,S_y\,T} + \frac{\lambda\,\Delta x}{2\,T}\right] \operatorname{erfc}\left[\sqrt{\frac{\lambda^2 t}{4\,S_y\,T}} + \sqrt{\frac{(\Delta x)^2 S_y}{4\,T\,t}}\right]\right\} \quad (6)$$

where $\lambda = K_S\, b\, / b_S$. It is assumed that the watertable remains above the base of the stream at all times (Rushton, 1999); i.e. the stream is of losing connected type (Brunner et al., 2011). The TGB and Hantush solutions are special cases of the Hunt (1999) ISD solution. The Hunt solution is equivalent to the TGB solution as $b_S \to 0$. The Hunt solution is equivalent to the Hantush solution if λ is instead parameterized as $\lambda = 2\,T/R = 2\,K_S\, b\, / b_S$.

Other ISD solutions addressed a range of unique hydrogeological conceptualisations. Unconfined conditions were most commonly simulated, although confined conditions were often assumed in order to simplify (i.e. linearize) governing equations. Solutions for leaky aquifers (Hunt, 2003; Butler et al. 2007; Zlotnik and Tartakovsky, 2008; Zlotnik, 2004) and multi-layer flow systems (Hunt, 2009; Ward and Lough, 2011; Ward and Falle, 2012) were also derived. Aquifer geometries considered included infinite (Hunt, 1999; Fox et al., 2002) or semi-infinite (Theis, 1941; Glover and Balmer, 1954; Hantush, 1965; Hunt, 2003), as well as rectangular (Chan, 1976; Huang et al., 2014, 2015), wedge-shaped (Chan et al., 1978; Yeh and Chang, 2006; Sedghi et al., 2009) or strip aquifers (Jenkins, 1968; Butler et al., 2001; Miller et al., 2007; Sun and Zhan, 2007; Zlotnik, 2014). Bore construction geometries considered included fully penetrating bores (Theis, 1941; Glover and Balmer, 1954; Hantush, 1965) and partially penetrating bores (Hunt, 1999; Zlotnik and Huang, 1999), as well as vertical and slanted bores (Tsou et al., 2010). Constant extraction rates were typically assumed, although transient extraction was also considered, including cyclic extraction schemes (Wallace et al., 1990; Darama, 2001). Streams were typically simulated as featuring a single linear geometry, but also included multiple parallel streams (Sun and Zhan, 2007), as well as curvilinear streams (Huang and Yeh, 2015) or right-angled streams (Hantush 1967). Variations in stream penetration extent were also considered, including full aquifer penetration (Theis, 1941; Glover and Balmer, 1954; Hantush, 1965) or partial aquifer penetration (Butler et al., 2001; Chen and Yin, 2004). Various representations of streambed conductance were applied, including the use of Dirichlet conditions to represent the absence of streambed conductance (Theis, 1941; Glover and Balmer, 1954). Alternatively, Cauchy or Robin conditions were used to represent variations in streambed thickness and permeability (Hantush, 1965; Hunt, 1999).

While many solutions assumed constant stream stage values, spatial and temporal variations in stream stages were also considered (Intaraprasong and Zhan, 2009; Neupauer et al., 2021). Solutions that considered streams featuring finite widths were derived by Butler et al. (2001) and Hunt (2008). In addition to their use as forward models for the prediction of instantaneous streamflow depletion, analytical ISD solutions have also been used to inversely estimate hydrogeological and streambed parameters. For example, Christensen (2000) and Lough and Hunt (2006) used the Hunt (1999) and Hunt (2003) ISD solutions, respectively, to inversely estimate aquifer transmissivity and specific yield, as well as a streambed conductance term. Implementations of analytical ISD solutions are readily available in software such as

STRMDEPL08 (Reeves, 2008) and the streamDepletr package for R (Zipper et al., 2019). In the following subsections, each of the TGB, Hantush, and Hunt solutions for ISD are reviewed in detail.

1.3. Numerical solutions for instantaneous streamflow depletion

1.3.1. Perturbation solutions

Numerical groundwater flow solutions are commonly used to assess ISD in contexts where sufficient data and/or subsurface complexity warrant the development of a numerical forward model. Numerical solutions feature far fewer assumptions than their analytical counterparts. For this reason, numerical solutions can be used to represent more complex conceptualisations and parameterizations, including irregular geometry and spatially heterogeneous parameters. Paired numerical forward models can be used to calculate ISD as the difference between aquifer–stream exchange fluxes using a perturbation approach.

The perturbation approach involves solving an appropriate form of the groundwater flow equation using a defined set of parameter values; e.g. from the minimization of discrepancies between modelled and measured flow system states. Additional solutions are then obtained for each perturbation of interest. For the specific case of streamflow depletion, additional solutions would be sought for each potential extraction well location. Instantaneous streamflow depletion is then calculated as the difference in aquifer–stream exchange flux between (1) the original model and (2) each perturbed model. When using the perturbation approach to assess ISD, the number of model runs required scales linearly with the number of potential extraction locations. More generally, the perturbation approach to calculating model sensitivities is efficient for well-posed inverse problems; i.e. when the number of potential states (whether forecast or hindcast) exceeds the number of variations (e.g. in parameters, or source/sink term locations) under consideration.

1.3.2. Adjoint solutions

For ill-posed problems, the adjoint state approach is more efficient than perturbation approaches. In most cases, the output of a single, additional adjoint model can be post-processed to obtain multiple state sensitivities. For the specific case of streamflow depletion metrics, the adjoint approach allows estimates of ISD to be calculated for all potential groundwater extraction locations using only two models: (1) the original forward model, and (2) one additional adjoint state model. The development of the adjoint state approach across various scientific and engineering disciplines is summarized as follows.

Use of the adjoint state approach to calculate the sensitivities of differential equations was first formalized for application to both linear and nonlinear systems by Cacuci (1981a, 1981b). This followed a number of diverse implementations in fields such as nuclear engineering (Wigner, 1945; Weinberg and Wigner, 1958; Gandini, 1967), reservoir engineering (Jacquard and Jain, 1965; Carter et al., 1974; Chavent et al., 1975) and meteorology (Marchuk, 1975). The adjoint state approach to sensitivity analysis and optimal control has been described in monographs such as Marchuk (1994), Cacuci (2003), and Cacuci et al. (2005). Adjoint state approaches were first applied to problems in groundwater hydrology by Vemuri and Karplus (1969), Neuman and Yakowitz (1979) and Neuman et al. (1980). The framework for the application of adjoint solutions to saturated groundwater flow problems was later derived for steady (Sykes et al. 1985) and for transient (Wilson and Metcalfe, 1985) flow conditions. The method was used to calculate the sensitivities of saturated (Townley and Wilson, 1985; Wilson and Metcalfe, 1985) and unsaturated (Kabala and Milly, 1990; Lehmann and Ackerer, 1997) groundwater flow solutions, and of solute transport solutions (Ahlfeld et al., 1988a, 1988b; Neupauer and Wilson 1999, 2001). Adjoint sensitivities were first derived for instantaneous streamflow depletion solutions by Neupauer and Griebling (2012) and Griebling and Neupauer (2013). The studies featured relatively complex, multi-layered hydrogeological flow systems featuring irregular geometries and nonlinear groundwater-surface water exchange mechanisms, as well as the evapotranspiration of shallow groundwater. The efficiency of the adjoint approach was shown to exceed that of the perturbation method by a factor of 250; i.e. by more than two orders of magnitude.

1.4. Cumulative streamflow depletion

The metric of instantaneous streamflow depletion represents the change in the volumetric rate of aquifer–stream exchange and therefore has units of $L^3.T^{-1}$. At a local scale this metric is appropriate, since it can be related to measurable rates of volumetric flow for processes located within both the stream and aquifer domains at a particular study location. However, conjunctive management of surface and groundwater resources at regional scales typically involves estimation of volumetric water balances, which are often averaged over finite (e.g. annual) time periods. This requires the integration of ISD through time, in order to estimate a total net annual volume, which can then be related to other water balance components. For this reason, an alternative metric of streamflow depletion was considered in the present study: cumulative stream depletion (CSD). This refers to the total volumetric reduction in flow from an aquifer to a stream (V_{CSD}) resulting from continuous groundwater extraction over a finite period (i.e. from t_0 to t_f), at the final time of extraction (t_f); i.e.:

$$V_{CSD}(t_f) = \int_{t_0}^{t_f} Q_{ISD}(t)\, dt = Q_B \int_{t_0}^{t_f} \frac{dQ_S(t)}{dQ_B}\, dt \qquad (7)$$

Cumulative stream depletion represents the cumulative volume of water that would otherwise have discharged to a stream in the absence of groundwater extraction. In comparison to the vast number of existing ISD solutions, solutions for the direct estimation of CSD do not currently existent, irrespective of whether they are solved analytically, semi-analytically, or numerically. In the present study, two new cumulative streamflow depletion solutions were derived: one closed-form analytical solution and one numerical adjoint solution. The analytical solution is suited to assessments of CSD in data poor areas or is suitable for didactic purposes. As a numerical solution, the adjoint solution features relatively fewer assumptions and is therefore suitable for assessments of CSD in data rich and/or hydrogeologically complex contexts. An additional key benefit of the adjoint solution is the ability to use a single numerical model to assess CSD resulting from any potential stressor location.

2. Methods

The numerical integration of analytical ISD solutions was used to provide benchmarks against which new analytical and numerical adjoint solutions were compared for three flow system conceptualizations. The Hunt (1999) analytical solution for ISD was used as the basis for derivation of a new closed-form analytical solution for CSD, which is appropriate for use in data poor investigations. A new numerical adjoint solution was also derived for the calculation of CSD, which is appropriate for use in data rich investigations. This was compared to both numerically integrated ISD solutions and the analytical CSD solution in a relatively simple application. The numerical adjoint CSD solution was also compared to numerical forward solutions in a relatively complex application.

2.1. Forward model

The governing equation for groundwater flow in an unconfined aquifer featuring stream–aquifer exchange and non-head-dependent flux boundary conditions (such as recharge) is:

$$S_y \frac{\partial h(\mathbf{x},t)}{\partial t} + \nabla \cdot [\mathbf{T}\, \nabla h(\mathbf{x},t)] - \frac{K_S}{b_S} A_S(\mathbf{x})[h(\mathbf{x},t) - h_S(\mathbf{x},t)] - Q_B\, \delta(\mathbf{x} - \mathbf{x}_B) \pm N(\mathbf{x},t) = 0 \tag{8}$$

where h is aquifer hydraulic head (L), h_s is stream stage (L), S_y is aquifer specific yield (unitless), $\mathbf{T}$ is a 3-D tensor of aquifer transmissivity (L^2.T^{-1}), K_s is streambed hydraulic conductivity (L.T^{-1}), b_s is streambed thickness perpendicular to the orientation of stream–aquifer exchange (L), A_s is a dimensionless function that has a value of unity along streams and zero elsewhere, N represents non-head-dependent source/sink terms such as recharge (L^3.T^{-1}), Q_B represents groundwater extraction (L^3.T^{-1}), and δ is a Dirac delta function. This equation can be solved using the boundary conditions:

$$h(\mathbf{x},t) = g_1(t) \text{ on } \Gamma_1 \tag{9}$$

$$\nabla h(\mathbf{x},t) \cdot \mathbf{n} = g_2(t) \text{ on } \Gamma_2 \tag{10}$$

$$[\alpha\, h\,(\mathbf{x},t) - \mathbf{T}\, \nabla h(\mathbf{x},t)] \cdot \mathbf{n} = g_3(t) \text{ on } \Gamma_3 \tag{11}$$

and the initial condition:

$$h(\mathbf{x}, t = t_0) = h_0(\mathbf{x}) \tag{12}$$

where α (L.T^{-1}) represents the parameterization of a Cauchy boundary condition.

2.2. Numerical integration of existing ISD solutions

The numerical integration of analytical ISD solutions provided a benchmark against which other solutions were compared. The Theis, Hantush and Hunt ISD solutions were numerically integrated using Clenshaw–Curtis quadrature, which was implemented using the SciPy library for Python (Virtanen et al., 2020). Absolute discrepancies were calculated as the arithmetic difference between the results of alternative methods and those of numerical integration. Percent difference discrepancies were expressed as a proportion of absolute discrepancies calculated by numerical integration.

2.3. Derivation of a new analytical solution for CSD

A closed-form solution for the total volume of cumulative streamflow depletion (V_{CSD}) resulting from continuous groundwater extraction over a finite period (i.e. from t_0 to t_f), at the final time of extraction (t_f) ,was derived through temporal integration of equation (6):

$$\begin{aligned} V_{CSD}(t_f) = \; Q_B \Bigg\{ & \left(2\,G^2 + t_f + \frac{1}{H^2} + \frac{2\,G}{H}\right) \operatorname{erfc}\left(\frac{G}{\sqrt{t_f}}\right) \\ & - \frac{e^{2\,G\,H + H^2 t_f}}{H^2} \; \operatorname{erfc}\left(\frac{G}{\sqrt{t_f}} + H\sqrt{t_f}\right) - \frac{2\,(G\,H+1)}{H\,\sqrt{\pi}} \sqrt{t_f}\; e^{-G^2/\,t_f} \\ & - \left(2\,G^2 + t_0 + \frac{1}{H^2} + \frac{2\,G}{H}\right) \operatorname{erfc}\left(\frac{G}{\sqrt{t_0}}\right) \\ & + \frac{e^{2\,G\,H + H^2 t_0}}{H^2} \; \operatorname{erfc}\left(\frac{G}{\sqrt{t_0}} + H\sqrt{t_0}\right) + \frac{2\,(G\,H+1)}{H\,\sqrt{\pi}} \sqrt{t_0}\; e^{-H^2/\,t_0} \Bigg\} \end{aligned} \tag{13}$$

where the coefficient G is defined as:

$$G = \sqrt{\frac{(\Delta x)^2\, S_y}{4\,K\,b}} \tag{14}$$

For the TGB case, the value of the H coefficient is equal to infinity. In practical terms, this means that all terms in equation (13) that are a function of H become zero-valued and can be omitted. For the Hunt case, the H coefficient is defined as:

$$H = \sqrt{\frac{\lambda^2}{4\,S_y\,K\,b}} \tag{15}$$

For the Hantush case, the lambda parameter is defined specifically as $\lambda = 2\ K_S\ b\ /b_S$; therefore, the H coefficient is defined as:

$$H = \sqrt{\frac{4\,{K_S}^2\ b^2}{b_S^2}\left(\frac{1}{4\,S_y\ K\ b}\right)} = \frac{K_S}{b_S}\sqrt{\frac{b}{S_y\ K}} \tag{16}$$

A comprehensive derivation of equation (13) is provided in Electronic Supplementary Material S1. If equation (13) can instead be applied as a function of time elapsed since the onset of extraction, rather than as a function of absolute time, then t_0=0 and all terms dependent on t_0 become zero-valued. Under these conditions, equation (6) simplifies to:

$$\begin{aligned} V_{CSD}(t_f) = Q_B \Bigg[& \left(2\,G^2 + t_f + \frac{1}{H^2} + \frac{2\,G}{H}\right) \operatorname{erfc}\left(\frac{G}{\sqrt{t_f}}\right) \\ & - \frac{e^{2\,G\,H + H^2 t_f}}{H^2} \operatorname{erfc}\left(\frac{G}{\sqrt{t_f}} + H\,\sqrt{t_f}\right) - \frac{2\,(G\,H+1)}{H\,\sqrt{\pi}}\,\sqrt{t_f}\ e^{-G^2/\,t_f} \Bigg] \end{aligned} \tag{17}$$

For a simplified conceptualization featuring a fully penetrating stream and bore in the absence of a stream bed conductance layer (i.e. which is consistent with the Theis-Glover-Balmer solution for ISD), equation (17) is not dependent on H and therefore simplifies further to:

$$V_{CSD}(t_f) = Q_B\ \left[\left(2\,G^2 + t_f\right) \operatorname{erfc}\left(\frac{G}{\sqrt{t_f}}\right) - \frac{2\,G\sqrt{t_f}\ e^{-G^2/t_f}}{\sqrt{\pi}}\right] \tag{18}$$

Equation (18) provides a useful upper limit for predictions of cumulative streamflow depletion. In particular, the assumptions of (a) full stream penetration and (b) zero streambed resistance will result in over-prediction of cumulative streamflow depletion, therefore ensuring that estimates are conservative.

To the authors' knowledge, these equations have not been derived previously. These expressions feature two dependent variables (i.e. Δx, t_f) and five parameters (K, S_y, b, K_s, Q_B), each of which are physically-based and are therefore measurable, or able to be estimated or constrained.

These equations can be implemented using scripted languages or spreadsheet software and will typically provide conservative predictions of maximum cumulative streamflow depletion, due to assumptions of full stream penetration extent, spatially uniform hydraulic properties, and (in the TGB case), the absence of a streambed conductance layer.

2.4. Numerical perturbation solution for CSD

The perturbation method of estimating cumulative streamflow depletion resulting from groundwater extraction at a given location and for a given duration involves the calculation of two solutions; i.e. representations of the flow system with and without the inclusion of the extraction term. The total volume of stream–aquifer exchange is calculated for each of (1) the reference case featuring zero extraction [i.e. $V_S\left(t_f; h\right)$] and (2) for the perturbed case featuring non-zero extraction [i.e. $V_S\left(t_f; h, \mathbf{x}_B\right)$]. Cumulative streamflow depletion can then be calculated as the difference between these two results as:

$$V_{CSD}\left(t_f\right) = V_S\left(t_f; h, \mathbf{x}_B\right) - V_S\left(t_f; h\right) \tag{19}$$

2.5. Numerical adjoint solution for CSD

The key benefit of the adjoint state approach is the ability to efficiently evaluate the volume of cumulative streamflow depletion resulting from extraction from a single bore at more than one potential location. Through the derivation of an appropriate adjoint model, V_{CSD} was calculated as a function of the adjoint state variable (ψ^*) which, for the present implementation, is dimensionless:

$$V_{CSD}\left(t_f\right) = Q_B \int_{t_f}^{t_0} \psi^*(t, \mathbf{x}_B)\, dt \tag{20}$$

where ψ^* is the solution to the adjoint equation, as defined below. Full details of the derivation of equation (20) are provided in Electronic Supplementary Material S2. This expression states that, for any given extraction bore location, the performance measure can be calculated as the temporal integral of the adjoint state variable at that location. Unlike equation (19), this solution avoids the computationally expensive calculation of the sensitivity of stream–aquifer exchange (Q_S) to extraction rate (Q_B), as required by the numerical perturbation approach (Section 2.4). For this reason, CSD resulting from extraction at any potential location $\mathbf{x}_B$ can be predicted using a single adjoint model. The governing equation for the adjoint model was defined as:

$$S_y \frac{\partial \psi^*(\mathbf{x},\tau)}{\partial \tau} + \nabla \cdot [\mathbf{T}\, \nabla \psi^*(\mathbf{x},\tau)] - \frac{K_S}{b_S} A_S(\mathbf{x})[\psi^*(\mathbf{x},\tau) - 1] = 0 \tag{21}$$

with boundary conditions:

$$\psi^*(\mathbf{x},\tau) = 0 \text{ on } \Gamma_1 \tag{22}$$

$$\nabla\psi^*(\mathbf{x},\tau) \cdot \mathbf{n} = 0 \text{ on } \Gamma_2 \tag{23}$$

$$[\alpha\, \psi^*(\mathbf{x},\tau) - \mathbf{T}\, \nabla\psi^*(\mathbf{x},\tau)] \cdot \mathbf{n} = 0 \text{ on } \Gamma_3 \tag{24}$$

and the terminal condition:

$$\psi^*(\mathbf{x},\tau = \tau_0) = 0 \tag{25}$$

where α (L.T^{-1}) represents the parameterization of a Cauchy boundary condition. To simplify the specification of the initial condition for the adjoint state model, the variable τ (which is equal to t_f–t) is used in place of t. Consequently, the adjoint state model is run backwards in time, from $\tau = \tau_0 = t_f$ (the final time) to $\tau = \tau_f = t_0$ (the initial time).

The form of the governing equation for the adjoint state model (equation 21) is similar to that of the forward model, with the following exceptions. Recharge was omitted, since it is not dependent on the rate of groundwater extraction. The groundwater extraction term itself was replaced by a value of unity, which was subsequently incorporated into the loading term. This source term (i.e. $(K_S/b_S)\, A_S(\mathbf{x})[\psi^*(\mathbf{x},\tau) - 1]$) was applied along the length of the stream(s) of interest and is commonly known as the "loading term" in adjoint state solutions. The formulation of this term is of conceptual interest, as it can identify the model inputs to which a specified model output is sensitive. The formulation of the loading term in the present study, and the insights that it provided, are discussed in Section 5.2. Due to the similar form of the adjoint state equation (21) to the forward equation (8), it can be solved using the same numerical scheme. In the present study, the finite-difference code MODFLOW-2005 (Harbaugh, 2005) was used to solve both forward and adjoint models.

Prior to numerical solution, a rescaling and offset was applied to the adjoint state variable. As described previously (Neupauer and Griebling, 2012; Griebling and Neupauer, 2013), there are two reasons for this adjustment. First, for certain parameter values, the magnitude of the loading term will be small with respect to numerical solution precision. Similarly, the spatial gradient of the adjoint state in the local vicinity of the loading term may also be small in relative terms. Therefore, a scaling parameter (i.e. γ) was used to increase the magnitude of the loading term. Second, depending upon the reference datum used in the vertical plane, the value of the loading term may be smaller than the specified bottom of aquifer elevation. Therefore, an offset parameter (i.e. β) was used to ensure that loading term values were always larger than bottom of aquifer elevations. The adjoint model state variable was therefore modified as: $\Psi^*(\mathbf{x},\tau) = \psi^*(\mathbf{x},\tau)\,\gamma + \beta$. The scaling parameter used here is the inverse of that used by Neupauer and Griebling (2012) and Griebling and Neupauer (2013). This alternative formulation was preferred as it better clarifies the linear transformation from ψ^* to Ψ^* during model pre-processing (and from Ψ^* to ψ^* during model post-processing).

Using a simple synthetic test case, the accuracy of the new analytical and numerical adjoint solutions for CSD were demonstrated through comparisons to an equivalent numerical forward model, as well as to the numerical integration of ISD analytical solutions for instantaneous streamflow depletion. The efficacy of the new numerical adjoint solution for the prediction of CSD in more complex contexts was subsequently demonstrated through application to a numerical groundwater flow model of the Gloucester River Basin alluvial aquifer in New South Wales, Australia.

3. Synthetic demonstration

Neupauer and Griebling (2012) (hereafter "N&G") presented a conceptual model to demonstrate an adjoint solution for instantaneous streamflow depletion. This was modified to facilitate comparisons to numerical integration of analytical solutions. Specifically, the two-sided N&G solution was simplified to a single-sided solution by using a Cauchy boundary condition (BC) to represent a stream on one side of the model domain (Figure 1). Dirichlet boundary conditions were specified on all other boundaries. Model outputs were checked to ensure that inflows did not occur through Dirichlet boundaries. This arrangement of boundary conditions was consistent with an infinite aquifer extent, as assumed by the analytical streamflow depletion solutions to which numerical model results were compared.

Initial hydraulic head values were set equal to the aquifer top elevation to avoid the desaturation of model cells. The stage parameter of the Cauchy boundary condition representing the stream was set equal to the aquifer top elevation to ensure equilibrium initial conditions, and therefore consistency with the analytical solutions to which results were compared. Streambed elevations were set equal to the base of the aquifer (i.e. 0 m), to ensure consistency with the assumption of full stream penetration extent used by the TGB and Hantush solutions. For the

TGB conceptualization, streambed hydraulic conductivity was specified equal to aquifer hydraulic conductivity. Conversely, for the Hantush conceptualization, streambed hydraulic conductivity was specified as three orders of magnitude smaller than aquifer hydraulic conductivity. Model outputs were generated at every time step. For adjoint state model simulations, scaling and offset variables were set to $\gamma = 10$ and $\beta = 100$ respectively. The effects of these parameters were subsequently removed during model post-processing.

All numerical solutions (both forward and adjoint) were computed using the finite difference flow simulator MODFLOW-2005 (Harbaugh, 2005). The model domain was discretized using spatially uniform cell dimensions of 50 m × 50 m × 50 m, resulting in a total of 100 rows and 100 columns. A simulated duration of 365 days was discretized using a uniform time step of 1 day, resulting in a total of 365 stress periods. The numerical solution was computed using the preconditioned conjugate gradient solver (Hill, 1990). Solver convergence criteria of 10^{-3} m and 10^{-3} $m^3.d^{-1}$ were specified for hydraulic head and flux calculations, respectively.

3.1. Results

For the conceptualization featuring a fully penetrating stream without a conductance layer present, numerical integration of the TGB ISD analytical solution (equation 4) was used as the basis for comparisons (Figure 2a-c). For the conceptualization featuring a fully penetrating stream with a conductance layer present, numerical integration of the Hantush ISD analytical solution (equation 5) was used (Figure 2d-f). For the conceptualization featuring a partially penetrating stream with conductance layer present, numerical integration of the Hunt ISD analytical solution was used (equation 6) (Figure 2g-i).

The analytical CSD solution was in near-exact agreement with the numerical integration of ISD solutions in all three conceptualizations (Figure 2a, 2d, 2g). In percentage terms, numerical CSD solutions were in near-exact agreement with numerical integration of ISD solutions when extraction occurred less than 3 km from the stream boundary condition (Figure 2b, 2e, 2h). However, these were associated with discrepancies of relatively small magnitude (Figure 2c, 2f, 2i). Therefore, in practical terms, these percent discrepancies were not substantial.

4. Real world case study

To demonstrate the suitability of the numerical adjoint approach for the estimation of cumulative streamflow depletion, the method was applied to an existing numerical groundwater flow model of the Gloucester Basin, Australia. Complexities in this model included an irregular domain and river system geometry, and time-varying rates of net recharge.

The Gloucester sedimentary basin is located approximately 200 km north-northeast of the city of Sydney in New South Wales, Australia. The region features a sub-tropical climate with a mean annual rainfall of 1100 mm and annual pan evaporation ranging from 1400 to 1700 mm. The Gloucester Basin contains up to 2500 m of faulted, deformed and eroded coal-bearing Permian sedimentary and volcanic rocks located along a sinuous north to northeast-oriented strike. The basin is entirely bounded by outcropping Carboniferous basement rocks. In the north of the basin the Avon River enters from the west and flows northward through the towns of Stratford and Gloucester before discharging into the Gloucester River at a confluence that also includes the Barrington River. Mean annual streamflow of 177×10^6 m^3 occurs in the Avon River. An alluvial aquifer associated with the Avon River served as the real-world case study for the present study. This aquifer is composed of Quaternary sediments ranging in size from clays to gravels, the total thickness of which ranged up to 15 m. Mean annual diffuse net recharge to the alluvial aquifer was estimated at 1 % of rainfall; i.e. 11 mm. Mean annual rates of evapotranspiration from shallow groundwater are estimated to range up to 50 % of rainfall; i.e. up to 550 mm. Watertable elevations are less than one metre below ground surface in locations proximal to the river. Under common flow conditions, the Avon River is characterised as a gaining system; i.e. local groundwater flows are consistently oriented toward the river and its tributaries. Limited extraction from the alluvial aquifer currently occurs for stock and domestic water supply (McVicar et al., 2014; Dawes et al., 2018; Peeters et al., 2018).

The spatial extent of the alluvial aquifer was discretized using a uniform grid of 225 rows and 140 columns (Figure 3a). A total of 3850 active cells were used for model calculations, with uniform dimensions of 90 m x 90 m. While the top and bottom elevations of model cells were variable, all cells featured a thickness (and therefore maximum saturated thickness) of 15 m. A period of 120 years of extraction was simulated, which was discretized using 1440 month-long steps. Hydraulic properties were represented using uniform values, with horizontal hydraulic conductivity = 1.0725 $m.d^{-1}$ and specific yield = 16 %. Time-varying net recharge was represented by applying a spatially distributed flux to each model cell, which ranged from 12 to 22 $mm.month^{-1}$. Groundwater discharge to the Avon River and its tributaries was represented using third-type (i.e. head-dependent) boundary conditions featuring a spatially uniform conductance value of 56 $m^2.d^{-1}$. (Peeters et al., 2018) (Figure 3a). Regional groundwater flow was oriented northwards and away from headwater areas (Figure 3b). All numerical solutions (both forward and adjoint) were computed using the finite difference flow simulator MODFLOW-2005 (Harbaugh, 2005), for which hydraulic head and flux convergence criteria of 10^{-3} m and 10^{-3} $m^3.d^{-1}$ were specified respectively. Model outputs were generated at every time step. Pre- and post-processing of model outputs was undertaken using the FloPy library for

Python (Bakker et al, 2016). Additional model information, including discretization and parameterization details, are listed in Table 1.

The prediction of interest for this case study was the volume of cumulative streamflow depletion resulting from groundwater extraction at a rate of 100 $m^3.d^{-1}$ (i.e. approximately equal to 1 $L.s^{-1}$) at a single bore located in any given cell in the model domain, other than the cells representing the Avon River and its tributaries. The numerical adjoint solution was used to provide these predictions across the model domain. For comparison, predictions at a subset of locations were calculated using the perturbation approach. For adjoint state model simulations, scaling and offset variables were set to γ=100 and β=200 respectively.

4.1. Results

Cumulative streamflow depletion volumes calculated from a total of 3850 models using the perturbation method ranged from near-zero values at model cells distant from the stream network (purple cells) to a maximum of 42.6×10^3 m^3 at model cells adjacent to the stream network (yellow cells) (Figure 4a). In comparison, CSD volumes calculated by a single adjoint state model ranged from near-zero values to 43.1×10^3 m^3 according to a consistent spatial structure (Figure 4b). Qualitative visual comparisons of adjoint state model results identified that orientations and magnitudes of spatial variations in CSD were consistent with perturbation method results.

Percent difference values (i.e. the discrepancy between adjoint and perturbation results, normalized by the latter results) ranged from –12 % to +75 % (Figure 5a). Arithmetic differences between perturbation and adjoint method results ranged from -2×10^3 m^3 to $+16\times10^3$ m^3 (Figure 5b). The signs of arithmetic and percentage discrepancies were in agreement across the majority of the model domain. Most locations featuring relatively large absolute percent difference values (i.e. >5 %) were coincident with relatively small absolute arithmetic differences (i.e. $<5\times10^3$ m^3). Exceptions included isolated areas where arithmetic differences were moderately large; i.e. $>5\times10^3$ m^3. These values were comparable in magnitude to the total volume of groundwater extracted over the simulated duration; i.e. approximately 4×10^3 m^3. These areas were predominantly located in the eastern half of the model domain, including in some headwater areas of the Avon River catchment. However, the arithmetic discrepancy values located in these areas were small with respect to the magnitudes of water balance components. The total volumes of inflow (primarily occurring as recharge) and outflow (primarily occurring as groundwater discharge to rivers) over the simulated duration of 120 years were in the order of $1{,}000{,}000\times10^3$ m^3. Therefore, a maximum arithmetic discrepancy in the order of $+16\times10^3$ m^3 represented a small fraction of the total water balance calculated over the simulated duration of 120 years.

5. Discussion

The results of the two case study applications are now discussed in terms of four themes, including the computational efficiency of the numerical adjoint method and insights derived from the parameterization of the loading term in the adjoint state solution. Assumptions and limitations of the numerical adjoint solution are recognized, and potential broader applications of the numerical adjoint solution are also proposed.

5.1. Computational efficiency

In practical terms, the primary advantage of the adjoint state approach to CSD estimation was the substantial reduction in computational time that was achieved by avoiding the need to run a unique forward model for every potential extraction location. For the Gloucester Basin flow model, each single forward model run required approximately five seconds to achieve numerical convergence. In addition, approximately 25 seconds were required for the automated pre- and post-processing of each model via a Python script. As the Gloucester Basin model contained 3850 active cells, the evaluation of all potential extraction locations using the perturbation approach required approximately 27 hours. In practice, the total time required when using the perturbation approach could be reduced through the use of parallel computing resources. In comparison, estimates of CSD resulting from all potential extraction locations were estimated simultaneously from a single numerical adjoint model run, which also required approximately five seconds to achieve numerical convergence. The comparatively high efficiency of the adjoint state approach is derived from the spatial integration (as implied in equation [21]) and temporal integration (as shown in equation [20]) used when defining the performance measure of interest.

5.2. Insights from the definition of the numerical adjoint loading term

An additional benefit of developing adjoint state solutions is the ability to derive closed-form expressions for the sensitivity of a specified model output to a specified model input. For closed-form analytical solutions, similar expressions can be derived through direct differentiation of the governing equation. For more complex models which require the solution of ordinary or partial differential equations, adjoint state solutions provide a similar benefit. In the present study, the loading term contained in the governing equation for the for the adjoint state (equation 21) was composed of two parameters: streambed hydraulic conductivity (K_s) and streambed thickness (b_s). In practice, when solving equation (21) the aquifer specific yield term is brought to the right-hand side; therefore, the loading term is effectively divided by aquifer specific yield (S_y). The identification of these significance of these three parameters (i.e. K_s , b_s and S_y) to the estimation of CSD was consistent with past studies. Sophocleous et al. (1995) used numerical models to demonstrate that fluxes through a third-type boundary (representing groundwater discharge to streams, for example) are most sensitive to the streambed conductance parameter. The presence of aquifer specific yield in the loading term is consistent with the influence of this parameter on the timing of responses to hydraulic perturbations more generally, as observed in pumping and slug test solutions (e.g. McElwee and Yukler, 1978).

5.3. Assumptions and limitations of the numerical adjoint CSD solution

It is widely acknowledged that making explicit the assumptions associated with a given model solution is best practice (Saltelli et al., 2013; Saltelli et al., 2020). Various simplified process representations were present in the Gloucester Basin forward model. A simplified representation of groundwater discharge to the Avon River and its tributaries was employed, based solely on the local stream-aquifer hydraulic gradient and mediated by a lumped conductance parameter. Additional necessary simplifications involved assuming that both (1) stream stage height and (2) unconfined aquifer saturated thickness were insensitive to extraction. However, both of these simplifications are common to many numerical groundwater flow models and are not unique to the numerical adjoint solution for CSD presented in this study.

The numerical adjoint method derived and presented in the present study does rely, however, on one key assumption: the linearity of the relationship between groundwater discharge responses to variations in groundwater extraction. The linearity of this driver–response relationship underpins the adjoint state approach, which is consistent with analytical ISD solutions. Specifically, the system response to a perturbation applied at the observation of interest (in the present study, the total reduction in groundwater discharge to a stream network, summed over time) is proportional to the system response resulting from a perturbation applied at the driver of interest (in the present study, groundwater extraction). The simulation of confined (rather than unconfined) aquifer conditions was required to ensure linearity, as was the linear parameterization of the third-type boundary conditions to represent groundwater discharge to the stream network.

5.4. Potential broader applications of the numerical adjoint CSD solution

The forward model also featured spatially uniform (and in some cases, isotropic) parameterizations of aquifer thickness, hydraulic conductivity, specific yield, and streambed conductance values. However, applications of the numerical adjoint solution are not limited to flow models featuring homogeneous parameterizations. Unlike many other performance functions assessed using groundwater flow models (e.g. Sykes et al., 1985; Metcalfe and Wilson, 1985), the expression used to calculate CSD (equation 20) is entirely a function of the adjoint state variable. It does not depend explicitly on the results of the forward model upon which the adjoint solution is based. Nor are adjoint-based calculations of CSD explicitly dependent upon the parameterization of hydraulic properties. For these reasons, the numerical adjoint solution for CSD presented here is also appropriate for application to models featuring heterogeneous parameterizations.

Two process representations were unique to the numerical adjoint solution, which related to (a) stream-aquifer interaction and (b) groundwater extraction. The Gloucester Basin flow model featured the representation of a perennial gaining stream network. The numerical adjoint solution is also appropriate for application to streams featuring non-monotonic interactions (i.e. fluctuations between gaining and losing type. Since the performance measure of interest (i.e. the volume of CSD) is a relative measure of change, it may represent any of: reductions in groundwater discharge to streams; a change from gaining to losing stream conditions; or an increase in aquifer recharge from streams. The key assumption here is that stream–aquifer exchanges remain fully hydraulically connected, irrespective of the extraction rate and duration applied.

In the present study, rates of groundwater extraction were assumed to be constant and uniform in time. The numerical adjoint solution presented here used the same temporal discretization scheme as the equivalent forward model. For this reason, the numerical adjoint solution presented is also appropriate to assess CSD resulting from discontinuous rates of groundwater extraction.

6. Conclusions

The traditional metric of streamflow depletion represents the instantaneous change in the volumetric rate of aquifer–stream exchange and is appropriate when applied at local scales. However, conjunctive management of surface and groundwater resources at regional scales typically involves estimation of volumetric water balances, which are often averaged over finite time periods. This requires a streamflow depletion metric that can be expressed as a total net annual volume, which can then be related to other water balance components. For this reason, an alternative metric of streamflow depletion was considered in the present study: cumulative stream depletion (CSD). This described the total volumetric reduction in flow from an aquifer to a stream resulting from continuous groundwater extraction over a finite period, at the final time of extraction.

A novel analytical solution for the prediction of CSD was derived, based upon a forward solution that accounted for streambed conductance and partial stream penetration. The solution can alternatively be parameterized to represent full stream penetration. A simplified version of the analytical solution was also presented, which excluded the effects of both partial stream penetration and streambed conductance. These analytical solutions for CSD are appropriate for use in data poor investigations and represent upper limits for CSD predictions.

Separately, a novel numerical solution for prediction of CSD was presented, based on the derivation and calculation of an adjoint state solution. The accuracy and efficiency of the numerical adjoint solution was demonstrated through applications to simple and complex groundwater flow models. Numerical adjoint solution results were compared to those obtained from both (a) forward numerical models and (b) the newly derived closed-form analytical solutions. In all cases, the accuracy of numerical adjoint solutions was demonstrated. The parameterization of the loading term used in the adjoint state solution identified three parameters of relevance to CSD prediction. These were streambed hydraulic conductivity and thickness, both of which contribute to the lumped parameterization of streambed conductance, as well as aquifer specific yield, which controls the rate at which hydraulic perturbations propagate through an aquifer. These findings were consistent with past sensitivity analyses of streamflow depletion solutions (e.g. Sophocleous et al., 1995) and interpretations of hydraulic testing.

The numerical adjoint method relied on the assumption that groundwater discharge responses to variations in groundwater extraction were linear. The simplified representation of unconfined conditions using confined flow was required to ensure linearity, as was the use of linear third-type boundary conditions to represent groundwater discharge to the stream network. For these reasons, the numerical adjoint approach to CSD is unsuitable for applications to circumstances in which linearized conditions are not met. These may include when extraction results in considerable variation in aquifer saturated thickness, or when stream-aquifer exchange fluxes are a nonlinear function of hydraulic gradient.

The computational advantage of the numerical adjoint solution was highlighted, where a single numerical model can be used to predict CSD impacts from all potential groundwater extraction locations in the vicinity of a gaining stream network. In comparison to the use of many forward models to calculate impacts by difference, the reduction in computational time required was equivalent to the number of potential extraction well locations. For the real-world case study presented, a substantial reduction in model run time of approximately 27 hours (i.e. a reduction of almost 100 %) was achieved. More generally, when the number of potential locations is large then similar reductions in model run times can be achieved when the adjoint state approach to CSD estimation is employed.

Acknowledgments

This research did not receive any specific grant from funding agencies in the public, commercial, or not-for-profit sectors. The authors thank Bob Anderssen his assistance in deriving an early version of the closed-form analytical solution for cumulative streamflow depletion. Funding of this work was supported by the Australian Commonwealth Government's Geological and Bioregional Assessments Program.

Supporting information

All scripts (as Python language scripts and as Jupyter Notebooks) and related datasets used to generate the results presented in this study can be obtained from the public GitHub code repository located at:

https://github.com/christurnadge/01_Streamflow_depletion_adjoint_sensitivity.

References

Ahlfeld, D. P., Mulvey, J. M., Pinder, G. F., and Wood, E. F. (1988a). Contaminated groundwater remediation design using simulation, optimization, and sensitivity theory: 1. Model development. Water Resources Research, 24(3), 431-441.

Ahlfeld, D. P., Mulvey, J. M., and Pinder, G. F. (1988b). Contaminated groundwater remediation design using simulation, optimization, and sensitivity theory: 2. Analysis of a field site. Water Resources Research, 24(3), 443-452.

Bakker, M., Post, V. E. A., Langevin, C. D., Hughes, J. D., White, J. T., Starn, J. J., and Fienen, M. N. (2016). Scripting MODFLOW model development using Python and FloPy. Groundwater, 54(5), 733-739.

Barlow, P. M., and Leake, S. A. (2012). Streamflow depletion by wells: Understanding and managing the effects of groundwater pumping on streamflow. U.S. Geological Survey Circular no. 1376, Reston, Virginia, USA, 84p.

Brunner, P., Cook, P. G., and Simmons, C. T. (2011). Disconnected surface water and groundwater: from theory to practice. Groundwater, 49(4), 460-467.

Butler, J. J., Zhan, X., and Zlotnik, V. A. (2007). Pumping-induced drawdown and stream depletion in a leaky aquifer system. Groundwater, 45(2), 178-186.

Butler, J. J., Zlotnik, V. A. and Tsou, M. S. (2001). Drawdown and stream depletion produced by pumping in the vicinity of a partially penetrating stream. Groundwater, 39(5), 651-659.

Cacuci, D. G. (1981a). Sensitivity theory for nonlinear systems. I. Nonlinear functional analysis approach. Journal of Mathematical Physics, 22(12), 2794-2802.

Cacuci, D. G. (1981b). Sensitivity theory for nonlinear systems. II. Extensions to additional classes of responses. Journal of Mathematical Physics, 22(12), 2803-2812.

Cacuci, D. G. (2003). Sensitivity and Uncertainty Analysis. Volume 1: Theory. CRC Press, London, UK, 285p.

Cacuci, D. G., Ionescu-Bujor, M., and Navon, I. M. (2005). Sensitivity and Uncertainty Analysis. Volume 2: Applications to Large-Scale Systems. CRC Press, London, UK, 367p.

Carter, R. D., Kemp Jr, L. F., Pierce, A. C., and Williams, D. L. (1974). Performance matching with constraints. Society of Petroleum Engineers Journal, 14(02), 187-196.

Chan, Y. K. (1976). Improved image-well technique for aquifer analysis. Journal of Hydrology, 29(1–2), 149-164.

Chan, Y. K., Mullineux, N., Reed, J. R., and Wells, G. G. (1978). Analytic solutions for drawdowns in wedge-shaped artesian aquifers. Journal of Hydrology, 36, 233-246.

Chavent, G., Dupuy, M., and Lemmonier, P. (1975). History matching by use of optimal theory. Society of Petroleum Engineers Journal, 15(01), 74-86.

Chen, X., and Yin, Y. (2004). Semianalytical solutions for stream depletion in partially penetrating streams. Groundwater, 42(1), 92-96.

Christensen, S. (2000). On the estimation of stream flow depletion parameters by drawdown analysis. Groundwater, 38(5), 726-734.

Darama, Y. (2001). An analytical solution for stream depletion by cyclic pumping of wells near streams with semipervious beds. Groundwater, 39(1), 79-86.

Dawes, W. R., Macfarlane, C., McVicar, T. R., Wilkes, P. G., Rachakonda, P. K., Henderson, B. L., Ford, J. H., Hayes, K. R., Holland, K. L., O'Grady, A. P., Marvanek, S. P., and Schmidt, R. K. (2018) Conceptual modelling for the Gloucester subregion: Product 2.3 for the Gloucester subregion from the Northern Sydney Basin Bioregional Assessment.

Department of the Environment and Energy, Bureau of Meteorology, CSIRO and Geoscience Australia, Australia, 124p.

Fox, G. A. (2004). Evaluation of a stream aquifer analysis test using analytical solutions and field data. Journal of the American Water Resources Association, 40(3), 755-763.

Fox, G. A., DuChateau, P., and Dumford, D. S. (2002). Analytical model for aquifer response incorporating distributed stream leakage. Groundwater, 40(4), 378-384.

Fox, G. A., Heeren, D. M., and Kizer, M. A. (2011). Evaluation of a stream-aquifer analysis test for deriving reach-scale streambed conductance. Transactions of the ASABE, 54(2), 473-479.

Gandini, A. (1967). A generalized perturbation method for bi-linear functionals of the real and adjoint neutron fluxes. Journal of Nuclear Energy, 21(10), 755-765.

Glover, R. E., and Balmer, G. G. (1954). River depletion resulting from pumping a well near a river. Eos, Transactions American Geophysical Union, 35(3), 468-470.

Griebling, S. A., and Neupauer, R. M. (2013). Adjoint modeling of stream depletion in groundwater-surface water systems. Water Resources Research, 49(8), 4971-4984.

Hantush, M. S. (1965). Wells near streams with semipervious beds. Journal of Geophysical Research, 70(12), 2829-2838.

Harbaugh, A. W. (2005). MODFLOW-2005, the US Geological Survey modular ground-water model: The ground-water flow process. Techniques and Methods report no. 6-A16, US Department of the Interior, U.S. Geological Survey, Reston, Virginia, USA, 253p.

Herron N. F., Crosbie, R. S., Viney, N. R., Peeters, L. J. M., and Zhang, Y. Q. (2018). Water balance assessment for the Gloucester subregion: Product 2.5 for the Gloucester subregion from the Northern Sydney Basin Bioregional Assessment. Department of the Environment and Energy, Bureau of Meteorology, CSIRO and Geoscience Australia, Australia, 40p.

Hill, M. C. (1990). Preconditioned conjugate-gradient 2 (PGC2), a computer program for solving groundwater flow equations. Water Resources Investigations report 90-4048, U.S. Geological Survey, Denver, Colorado, USA, 43p.

Huang, C. S., and Yeh, H. D. (2015). Estimating stream filtration from a meandering stream under the Robin condition. Water Resources Research, 51, 4848-4857.

Huang, C. S., Lin, W. S., and Yeh, H. D. (2014). Stream filtration induced by pumping in a confined, unconfined or leaky aquifer bounded by two parallel streams or by a stream and an impervious stratum. Journal of Hydrology, 513, 28-44.

Huang, C. S., Yang, T., and Yeh, H. D. (2018). Review of analytical models to stream depletion induced by pumping: Guide to model selection. Journal of Hydrology, 561, 277-285.

Huang, C.S., Yang, S.Y., and Yeh, H.D. (2015). Technical Note: Approximate solution of transient drawdown for constant-flux pumping at a partially penetrating well in a radial two-zone confined aquifer. Hydrology and Earth System Sciences, 19, 2639-2647.

Hunt, B. (1999). Unsteady stream depletion from ground water pumping. Groundwater, 37(1), 98-102.

Hunt, B. (2003). Unsteady stream depletion when pumping from semiconfined aquifer. Journal of Hydrologic Engineering, 8(1), 12-19.

Hunt, B. (2008). Stream depletion for streams and aquifers with finite widths. Journal of Hydrologic Engineering, 13(2), 80-89.

Hunt, B. (2009). Stream depletion in a two-layer leaky aquifer system. Journal of Hydrologic Engineering, 14(9), 895-903.

Hunt, B. (2014). Review of stream depletion solutions, behavior, and calculations. Journal of Hydrologic Engineering, 19(1), 167-178.

Intaraprasong, T., and Zhan, H. B. (2009). A general framework of stream-aquifer interaction caused by variable stream stages. Journal of Hydrology, 373(12), 112-121.

Jacquard, P. and Jain, C. (1965). Permeability distribution from field pressure data. Society of Petroleum Engineers Journal, 5(04), 281-294.

Jenkins, C. T. (1968). Techniques for computing rate and volume of stream depletion by wells. Groundwater, 6(2), 37-46.

Kabala, Z. J., and Milly, P. C. D. (1990). Sensitivity analysis of flow in unsaturated heterogeneous porous media: Theory, numerical model, and its verification. Water Resources Research, 26(4), 593-610.

Lehmann, F., and Ackerer, P. (1997). Determining soil hydraulic properties by inverse method in one-dimensional unsaturated flow. Journal of Environmental Quality, 26(1), 76-81.

Lough, H. K., and Hunt, B. (2006). Pumping test evaluation of stream depletion parameters. Groundwater, 44(4), 540-546.

Marchuk, G. I. (1975). Formulation of the theory of perturbations for complicated models. Applied Mathematics and Optimization, 2(1), 1-33.

Marchuk, G. I. (1994). Adjoint equations and analysis of complex systems. Kluwer Academic Publishers, Boston, Massachusetts, USA, 466p.

McElwee, C. D., and Yukler, M. A. (1978). Sensitivity of groundwater models with respect to variations in transmissivity and storage. Water Resources Research, 14(3), 451-459.

McVicar, T. R., Langhi, L., Barron, O. V., Rachakonda, P. K., Zhang, Y. Q., Dawes, W. R., MacFarlane, C., Holland, K. L., Wilkes, P. G., Raisbeck-Brown, N., Marvanek, S. P., Li,

L. T., and Van Niel, T. G. (2014). Context statement for the Gloucester subregion: Product 1.1 from the Northern Sydney Basin Bioregional Assessment. Department of the Environment, Bureau of Meteorology, CSIRO and Geoscience Australia, Australia, 104p.

Mehl, S., and Hill, M. C. (2010). Grid-size dependence of Cauchy boundary conditions used to simulate stream–aquifer interactions. Advances in Water Resources, 33(4), 430-442.

Miller, C. D., Durnford, D., Halstead, M. R., Altenhofen, J., and Flory, V. (2007). Stream depletion in alluvial valleys using the SDF semianalytical model. Groundwater, 45(4), 506-514.

Neuman, S. P., and Yakowitz, S. (1980). A statistical approach to the inverse problem of aquifer hydrology: 1. Theory. Water Resources Research, 15(4), 845-860.

Neuman, S. P., Fogg, G. E., and Jacobson, E. A. (1980). A statistical approach to the inverse problem of aquifer hydrology: 2. Case study. Water Resources Research, 16(1), 33-58.

Neupauer, R. M., and Griebling, S. A. (2012). Adjoint simulation of stream depletion due to aquifer pumping. Groundwater, 50(5), 746-753.

Neupauer, R. M., and Wilson, J. L. (1999). Adjoint method for obtaining backward-in-time location and travel time probabilities of a conservative groundwater contaminant. Water Resources Research, 35(11), 3389-3398.

Neupauer, R. M., and Wilson, J. L. (2001). Adjoint-derived location and travel time probabilities for a multidimensional groundwater system. Water Resources Research, 37(6), 1657-1668.

Neupauer, R.M., Lackey, G. D., and Pitlick, J. (2021). Exaggerated stream depletion in streams with spatio-temporally varying streambed conductance. Journal of Hydrologic Engineering, 26(2), 04020066, doi:10.1061/(ASCE)HE.1943-5584.0002043.

Peeters, L. J. M., Dawes, W. R., Rachakonda, P. R., Pagendam, D. E., Singh, R. M., Pickett, T. W., Frery, E., Marvanek, S. P., and McVicar, T. R. (2018). Groundwater numerical modelling for the Gloucester subregion: Product 2.6.2 for the Gloucester subregion from the Northern Sydney Basin Bioregional Assessment. Department of the Environment and Energy, Bureau of Meteorology, CSIRO and Geoscience Australia, Australia, 160p.

Reeves, H. W. (2008). STRMDEPL08-An extended version of STRMDEPL with additional analytical solutions to calculate streamflow depletion by nearby pumping wells. Open-File Report 2008-1166, U.S. Geological Survey, Reston, Virginia, U.S.A., 22p.

Rushton, K. (1999). Discussion of "Unsteady stream depletion from ground water pumping" by B. Hunt. Groundwater, 37(6), 805.

Saltelli, A., Bammer, G., Bruno, I., Charters, E., Di Fiore, M., Didier, E., Espeland, W. N., Kay, J. Lo Piano, S., and Mayo, D. (2020). Five ways to ensure that models serve society: A manifesto. Nature, 582, 482–484.

Saltelli, A., Guimaraes Pereira, Â., Van der Sluijs, J. P., and Funtowicz, S. (2013). What do I make of your latinorum? Sensitivity auditing of mathematical modelling. International Journal of Foresight and Innovation Policy, 9(2-3-4), 213-234.

Sedghi, M. M., Samani, N., and Sleep, B. (2009). Three-dimensional semi-analytical solution to groundwater flow in confined and unconfined wedge-shaped aquifers. Advances in Water Resources, 32(6), 925-935.

Sophocleous, M., Koussis, A., Martin, J. L., and Perkins, S. P. (1995). Evaluation of simplified stream-aquifer depletion models for water rights administration. Groundwater, 33(4), 579-588.

Sun, D. M., and Zhan, H. B. (2007). Pumping induced depletion from two streams. Advances in Water Resources, 30(4), 1016-1026.

Sykes, J. F., Wilson, J. L., and Andrews, R. W. (1985). Sensitivity analysis for steady state groundwater flow using adjoint operators. Water Resources Research, 21(3), 359-371.

Theis, C. V. (1941). The effect of a well on the flow of a nearby stream. Eos, Transactions American Geophysical Union, 22(3), 734-738.

Townley, L. R., and Wilson, J. L. (1985). Computationally efficient algorithms for parameter estimation and uncertainty propagation in numerical models of groundwater flow. Water Resources Research, 21(12), 1851-1860.

Tsou, P. R., Feng, Z. Y., Yeh, H. D., and Huang, C. S. (2010). Stream depletion rate with horizontal or slanted wells in confined aquifers near a stream. Hydrology and Earth System Sciences, 14(8), 1477-1485.

Vemuri, V., and Karplus, W. J. (1969). Identification of nonlinear parameters of ground water basins by hybrid computation. Water Resources Research, 5(1), 172-185.

Virtanen, P., Gommers, R., Oliphant, T. E., Haberland, M., Reddy, T., Cournapeau, D., Burovski, E., Peterson, P., Weckesser, W., Bright, J., van der Walt, S. J., Brett, M., Wilson, J., Millman, K. J., Mayorov, N., Nelson, A. R. J., Jones, E., Kern, R., Larson, E., Carey, . J., Polat, I., Feng, Y., Moore, E. W., VanderPlas, J., Laxalde, D., Perktold, J., Cimrman, R., Henriksen, I., Quintero, E. A., Harris, C. R., Archibald, A. M., Ribeiro, A. H., Pedregosa, F., and Van Mulbregt, P. (2020). SciPy 1.0: Fundamental algorithms for scientific computing in Python. Nature Methods, 17(3), 261-272.

Wallace, R. B., Darama, Y., and Annable, M. D. (1990). Stream depletion by cyclic pumping of wells. Water Resources Research, 26(6), 1263-1270.

Ward, N. D., and Falle, S. (2012). Simulation of a multilayer leaky aquifer with stream depletion. Journal of Hydrologic Engineering, 18(6), 619-629.

Ward, N. D., and Lough, H. (2011). Stream depletion from pumping a semiconfined aquifer in a two-layer leaky aquifer system. Journal of Hydrologic Engineering, 16(11), 955-959.

Weinberg, A. M. and Wigner, E. P. (1958). The Physical Theory of Neutron Chain Reactors. University of Chicago Press, Chicago, Illinois, USA, 801p.

Wigner, E. P. (1945). Effect of small perturbations on pile period. Manhattan Project Report CP-G-3048.

Wilson, J. L., and Metcalfe, D. E. (1985). Illustration and verification of adjoint sensitivity theory for steady state groundwater flow. Water Resources Research, 21(11), 1602-1610.

Yeh, H. D., and Chang, Y. C. (2006). New analytical solutions for groundwater flow in wedge-shaped aquifers with various topographic boundary conditions. Advances in Water Resources, 29(3), 471-480.

Zipper, S. C., Gleeson, T., Kerr, B., Howard, J. K., Rohde, M. M., Carah, J., and Zimmerman, J. (2019). Rapid and accurate estimates of streamflow depletion caused by groundwater pumping using analytical depletion functions. Water Resources Research, 55(7), 5807-5829.

Zlotnik, V. A. (2004). A concept of maximum stream depletion rate for leaky aquifers in alluvial valleys. Water Resources Research, 40(6).

Zlotnik, V. A. (2014). Analytical methods for assessment of land-use change effects on stream runoff. Journal of Hydrologic Engineering, 20(7), 06014009-1–06014009-5.

Zlotnik, V. A., and Huang, H. (1999). Effect of shallow penetration and streambed sediments on aquifer response to stream stage fluctuations (analytical model). Groundwater, 37(4), 599-605.

Zlotnik, V. A., and Tartakovsky, D. M. (2008). Stream depletion by groundwater pumping in leaky aquifers. Journal of Hydrologic Engineering, 13(2), 43-50.

Figures

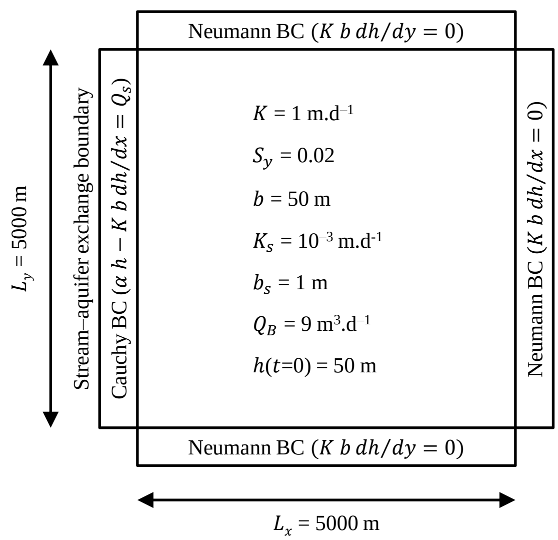

Figure 1. Synthetic groundwater flow model boundary conditions, initial condition, and parameterization.

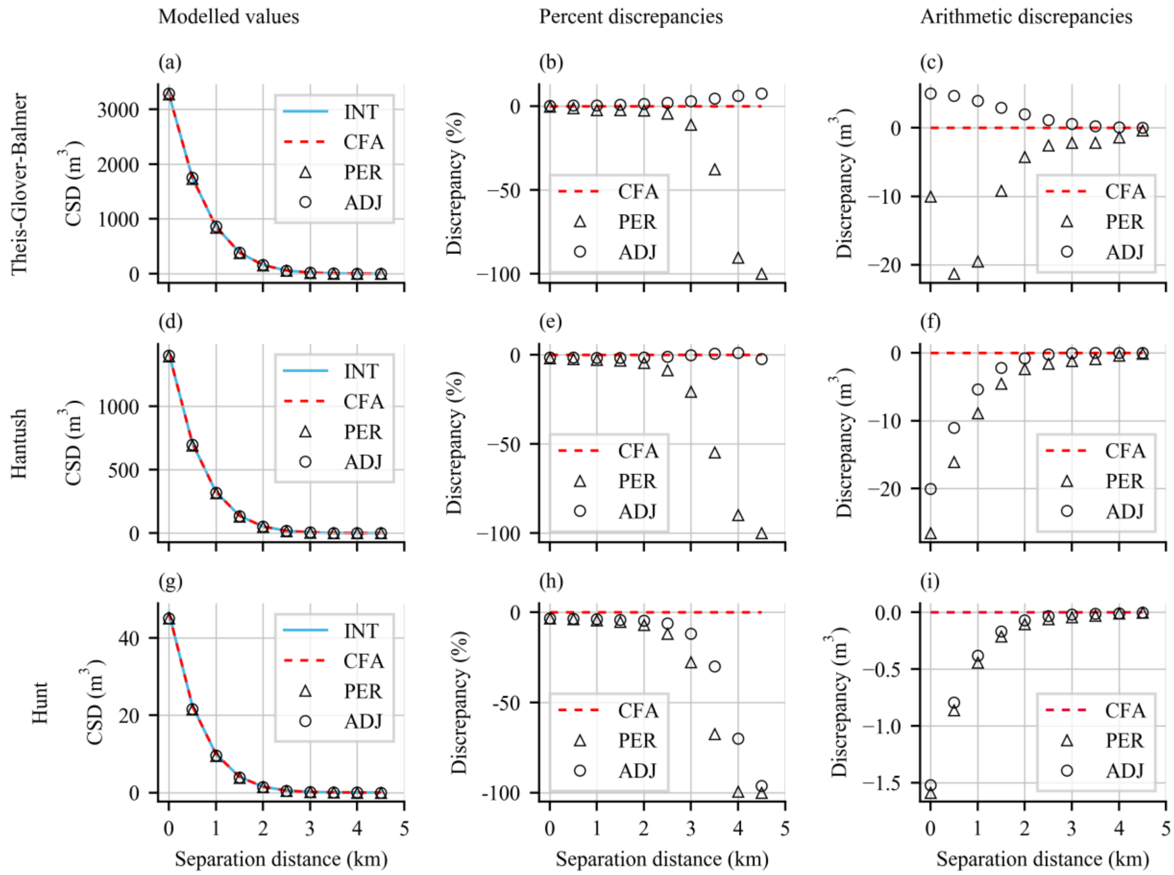

Figure 2. Analytical and numerical solutions for cumulative streamflow depletion (first column) and corresponding discrepancies with respect to numerical integration of ISD solutions, in percentage terms (second column) and as raw values (third column). All results are presented as functions of bore-stream separation distance. (a-c) streambed conductance layer absent (Theis-Glover-Balmer conceptualization); (d-f) streambed conductance layer present (Hantush conceptualization); (g-i) streambed conductance layer present and stream partially penetrating the aquifer (Hunt conceptualization). Extraction bore to stream distances were oriented perpendicular to the stream orientation. Abbreviations used: INT=numerical integration of analytical ISD solution; CFA=closed-form analytical CSD solution; PER=numerical perturbation-based solution; ADJ=numerical adjoint state solution, TGB=Theis-Glover-Balmer solution.

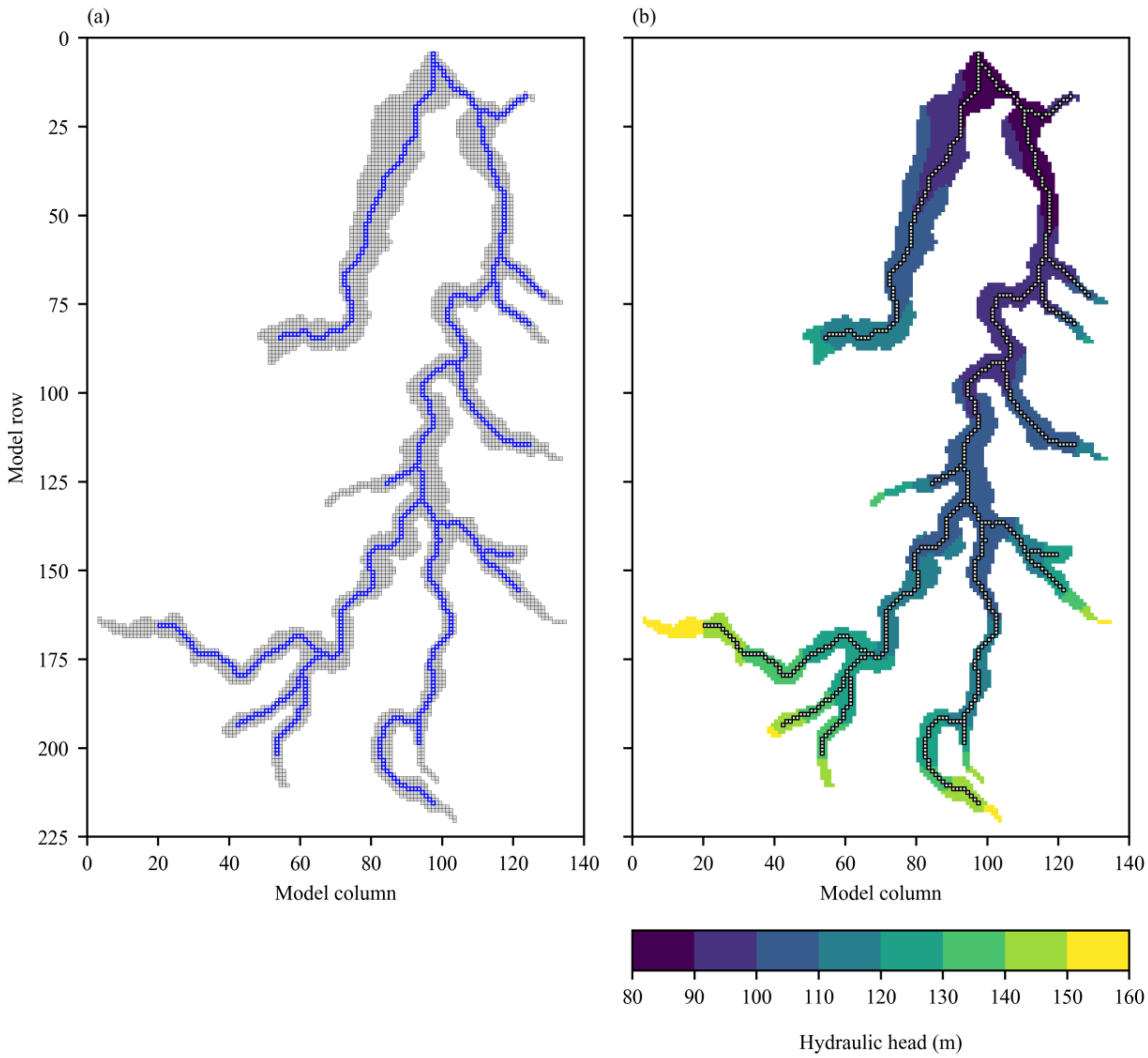

Figure 3. Numerical groundwater flow model of the Gloucester Basin alluvial aquifer. (a) Spatial discretization, with active cells shown in grey and stream boundary conditions shown in blue. (b) Spatial distribution of hydraulic head calculated by the forward model after 120 years of simulation.

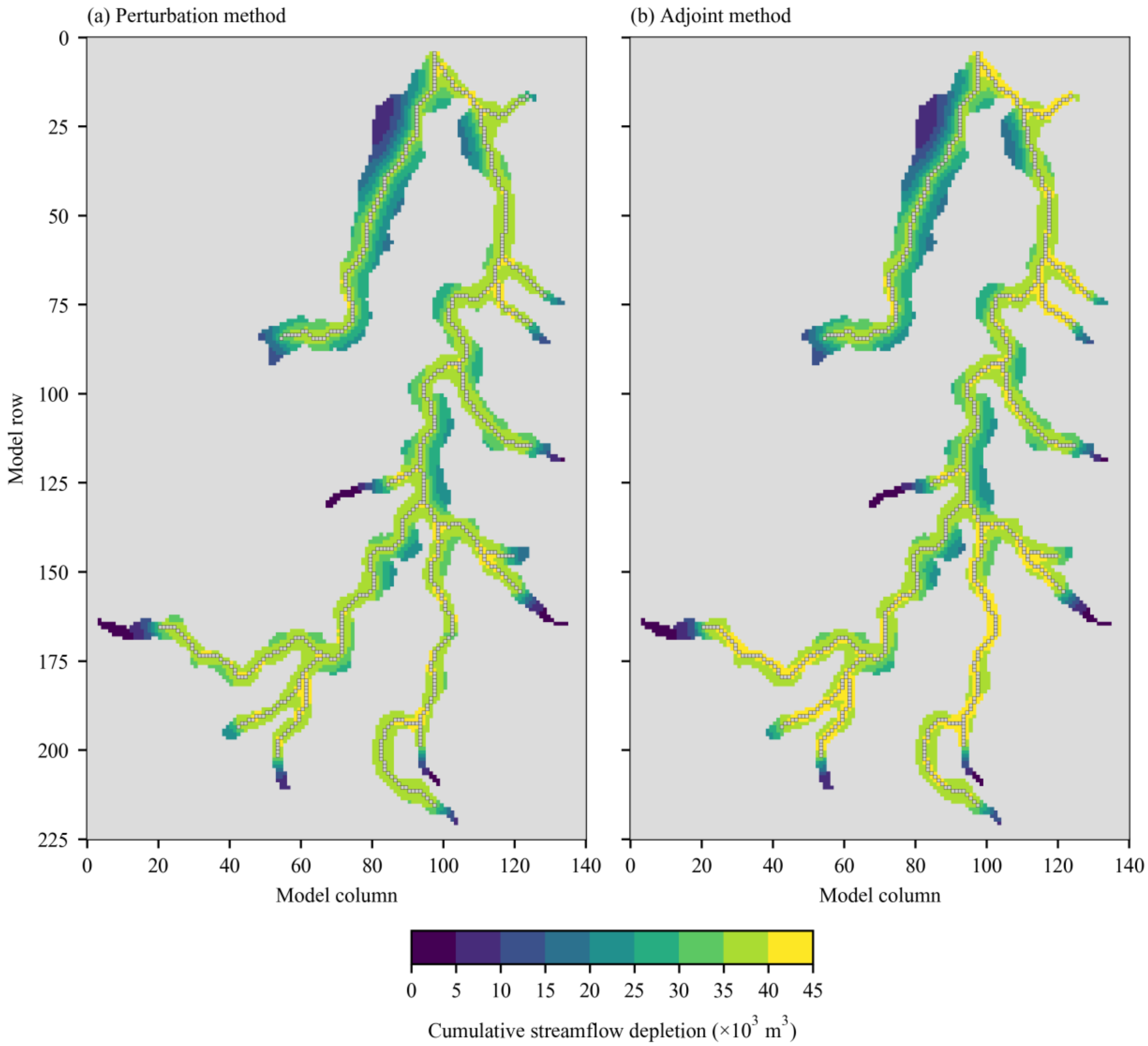

Figure 4. (a) Cumulative streamflow depletion volumes resulting from single bore extraction in the Gloucester Basin calculated via the perturbation method using 3850 forward model runs. (b) Equivalent results calculated via an adjoint state solution using a single model run. Model cells representing the Avon River network are presented as grey open squares for context.

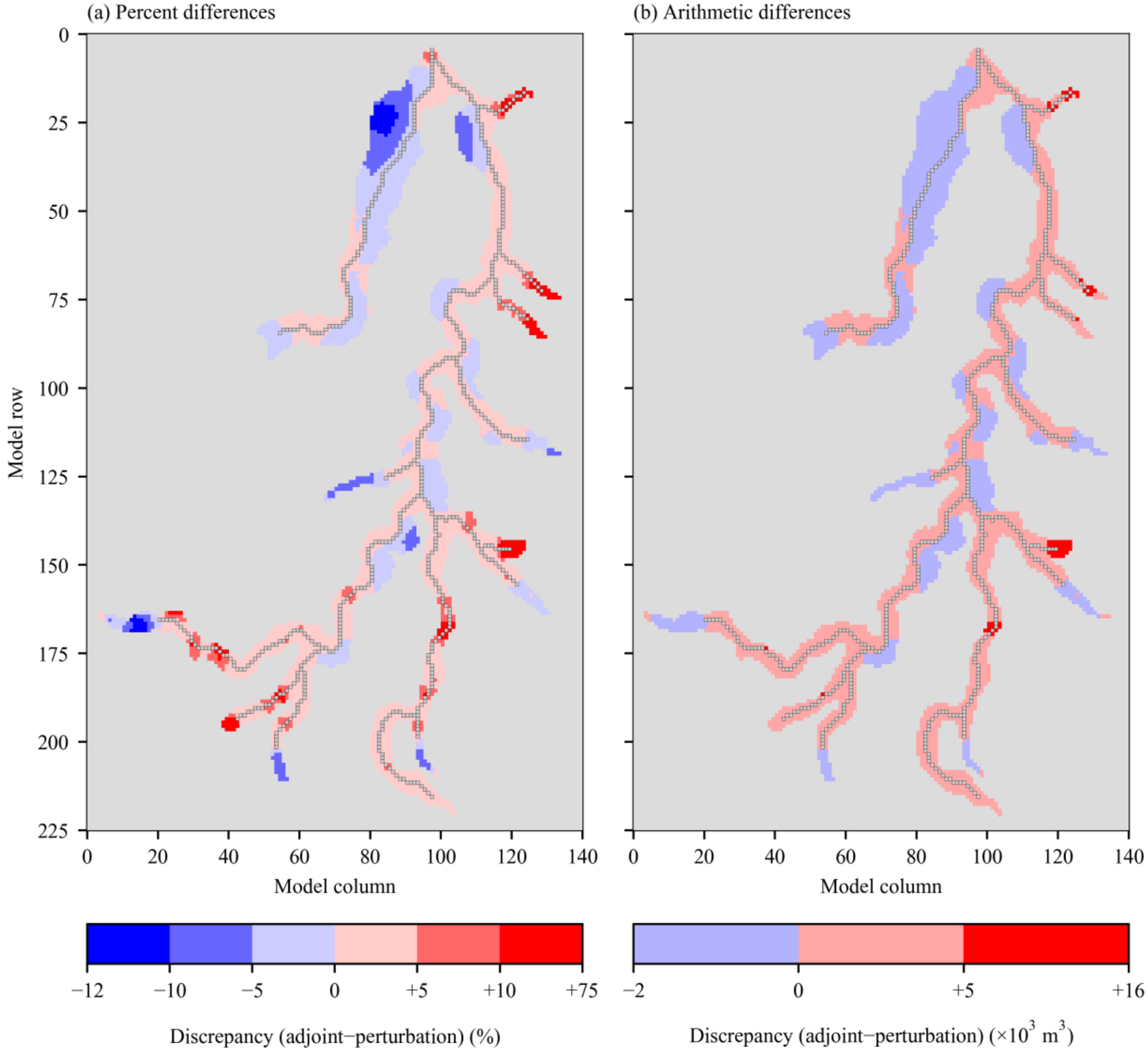

Figure 5. (a) Discrepancies between cumulative streamflow depletion volumes calculated via the perturbation and adjoint state methods, expressed as percentage differences. (b) Discrepancies expressed instead as arithmetic differences. Model cells representing the Avon River network are presented as grey open squares for context. Note: non-uniform color bar bin sizes were used to maximize figure clarify.

Tables

Table 1. Gloucester Basin groundwater flow model summary, including discretization and parameterization details.

Parameter	Value	Units
Spatial extent (x,y)	20.25 × 12.60	km
Model cell size (x,y)	90 × 90	m
Spatial extent (z)	15	m
Model cell size (z)	15	m
Temporal extent	120	y
Time step length	30.4375	d
Number of active cells	3850	cells
Aquifer hydraulic conductivity, K	16	m.d^{-1}
Aquifer specific yield, S_y	1	%
Streambed conductance, C_s	56	m^2.d^{-1}
Extraction flux, Q_B	100	m^3.d^{-1}

Table 2. Table of symbols used

Symbol	**Units**	**Description**
A_s	–	Dimensionless function with a value of unity along streams and zero elsewhere
b	L	Aquifer saturated thickness
b_S	L	Streambed thickness
C_S	L^2.T^{-1}	Streambed conductance
G	–	$\sqrt{\left[(\Delta x)^2\ S_y\right]/(4\ K\ b)}$
H	–	$\sqrt{\lambda^2/\left(4\ S_y\ K\ b\right)}$
h	L	Aquifer hydraulic head
h_S	L	Stream stage height
K	L.T^{-1}	Aquifer hydraulic conductivity
K_S	L.T^{-1}	Stream bed hydraulic conductivity
L_x	L	Numerical model domain extent in x-plane
L_y	L	Numerical model domain extent in y-plane
N	L^3.T^{-1}	Source/sink term used in governing equation for saturated groundwater flow
Q_B	L^3.T^{-1}	Volumetric rate of bore extraction
Q_S	L^3.T^{-1}	Volumetric rate of aquifer–stream exchange
Q_{ISD}	L^3.T^{-1}	Volumetric rate of instantaneous streamflow depletion
R	L	$K\ B_S/K_S$

Symbol	Units	Description
S_y	–	Aquifer specific yield
T	$\mathrm{L}^2.\mathrm{T}^{-1}$	Aquifer transmissivity
t_f	T	Final time; i.e. at which groundwater extraction ceases
W_S	L	Streambed width
V_{CSD}	L^3	Cumulative streamflow depletion volume
V_S	L^3	Total volume of stream–aquifer exchange
$\mathbf{x}_B$	[L, L]	Bore location vector
α	$\mathrm{L}^2.\mathrm{T}^{-1}$	Cauchy boundary condition parameter
β	–	Adjoint state variable offset parameter for numerical simulation
γ	–	Adjoint state variable scaling parameter for numerical simulation
λ	L	Streambed leakance
ψ^*	–	Adjoint state variable
Ψ^*	–	Scaled and offset adjoint state variable for numerical simulation
τ	T	Backwards time, with respect to the final time of simulation; i.e. $\tau = t - t_f$